Effects of coating fluorapatite on Ti-6Al-4V by Nd-YAG laser cladding

C.S. Chien[1], T.Y. Liao[2], T.F. Hong[3], T.Y. Kuo*[2], J.L.Wu[4], Y.T. Cheng [2]

[1] *Chimei Foundation Hospital, Tainan 710, TAIWAN, ROC*

[2] *Department of Mechanical Engineering, Southern Taiwan University, Tainan 710, TAIWAN, ROC*
**E-mail: tykuo@mail.stut.edu.tw *Corresponding author*

[3]*Department of Materials Engineering, National Pingtung University of Science and Technology, Pingtung 912, TAIWAN, ROC*

[4]*Department of Mechanical Engineering, National Cheng Kung University, Tainan 701, TAIWAN, ROC*

Abstract

Hydroxyapatite (HA) has been commonly applied on the surface of biomedical implants via plasma spraying or pulsed laser deposition method. However, the bonding strength between the coating layer and the substrate generated by these methods is relatively low. The high temperature process also usually causes the structural unstable of HA, and then degrades the bioactivity and survive duration of the coating layer after the following implantation. Fluorapatite (FA) is chosen as the coating material in the study due to its better structural stability and lower solubility. Polyvinyl alcohol (PVA) and sodium silicate (WG) are selected as a binder material to mixed with FA, respectively, and is then clad on Ti-6Al-4V substrates using an Nd-YAG laser beam. Hardness test, microscopy and XRD analysis are utilized to evaluate the bonding quality of the coating layer under different processing parameters. The results show that a metallurgical bonding layer with better quality can be achieved by Nd-YAG laser cladding technique.

Keywords: *Laser cladding, Hydroxyapatite, Fluorapatite, Ti-6Al-4V.*

Introduction

Cementless method is one of the artificial hip joint immobilization techniques to the host tissue nowadays [1]. Hydroxyapatite (HA, $Ca_{10}(PO_4)_6(OH)_2$) is normally used as a bioactive coating material on metallic implant (e.g. Titanium and its alloys) surfaces to generate chemical bonds between implant and surrounding bone tissue for achieving the immobilization effect following implantation.

HA coating techniques, such as plasma spraying, sol-gel coating, electrochemical, pulsed laser deposition methods [2-5], are mainly considered for the biomedical implants usage. However, some of these methods generate a mechanical rather than metallurgical bonding between the coating and substrate, and hence the bonding strength is relatively low. The coating tends to crack and detach from the metallic implant surfaces due to the large mismatch in their thermal expansion coefficient [6,7]. In addition, when the process is carried out under a high temperature, the phase transformation is easily found of the coated HA, and hence effects its crystallinity, stability and bioactivity [8,9]. Fluorapatite (FA, $Ca_5(PO_4)3F$) possesses a potential advantage over HA with its higher chemical stability and aptitude to delay caries process without the biocompatibility degradation. It is known that the fluorine ion itself protects dental and bone caries and also enhances mineralization and crystallization. Studies [10,11] also show that FA has a better resistance than HA in an acid solution less than pH 3 or body fluid, due to its smaller lattice parameter. FA has shown good phase stability even at higher temperature [12]. Because of these advantages over HA, FA starts to be applied as an advanced coating material recently [13,14].

In the study, FA was chosen as a coating material mixed with polyvinyl alcohol (PVA, $(C_2H_4O)n$) [15] and water glass (WG, $Na_2O \cdot nSiO_2$) [16], respectively, and then clad the mixture on Ti-6Al-4V substrates using an Nd-YAG laser beam. A series of experiments are then performed to investigate the effects of the binder, the laser processing parameters on the morphology, Ca/P ratio and hardness of the various coatings.

Experimental Procedure

The Fluorapatite powers used in the present study was supplied by Showa Inc., Japan. FA was mixed with a binder material (either PVA or WG) by 50:50 in weight % and then well stirred into slurry. The chemical composition of the Ti-6Al-4V alloy used in the present experiments is shown in Table 1. Substrates for the laser cladding process were prepared by machining the Ti-6Al-4V alloy into thin plates with dimensions of 100 mm × 60 mm × 3.8 mm. Following a drying process, the samples were laser clad using an Nd-YAG laser set to a continuous wave mode under two different output powers. The laser cladding experiments were conducted in an Ar shielded atmosphere (Ar flow rate: 25 l/min) using a 5° incident angle and a 15 mm defocus length. The experimental parameters and setup are shown in Table 2, respectively. The microstructures of the clad specimens were characterized via scanning electron microscopy (SEM). The Ca/P ratio of the coating layer was calculated from the atomic percentage of Ca and P in the structure measured by energy dispersive X-ray spectrometer (EDS) equipped in SEM. The phases of transition layer were analyzed by X-Ray diffractometry (XRD). The microhardness of the weld beads was measured by a Vickers automatic microhardness tester using a load of 300g.

Table 1. Chemical composition (wt-%) of Ti-6Al-4V.

Al	V	O	Fe	C	N	H	Ti
6.1	4.24	0.152	0.16	0.017	0.008	0.0006	Bal.

Table 2. Parameters used in Nd-YAG laser cladding process.

Power (W)	Travel Speed (mm/min)	Pre-place Thickness (mm)
740	300	0.8
1150		

Results and Discussion

1. Morphology and microstructure of weld beads

Figure 1 shows the cross-section OM image of the weld beads under various binder and output power conditions. The weld bead comprises three distinct regions, namely the coating layer , the transition layer and substrate (Figure 2)., respectively. It is observed that the transition layer of the WG sample is thinner than the one of PVA sample under the same laser processing condition, and it is increased with the output power. This is most likely the result of the difference in the melting temperatures of the two binders, i.e. 1300°C for WG and 240°C for PVA. A larger input energy needs to be consumed for melting a binder with higher melting temperature, and this causes a less energy allowed to penetrate further forming a thinner transition layer.

Figure 3 shows the morphology of coating layers processed at various conditions. The figures reveal that when a relative low output power (740W) was used, the coating layer was composed by a coral- and dendrite-like structure in the PVA sample; whereas dendrite structure was mainly found in the WG counterpart. The microstructure of the layers was getting coarser with the increase of output power. In addition, they are all composed by fine porous structures, and it is believed that helpful for Ca ions or bone cells attraction and attachment following implantation.

Power (W)	Weld Bead Profile	
	PVA	WG
740	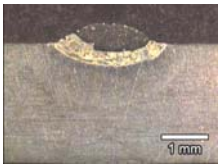	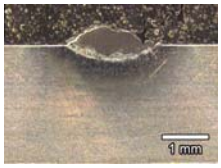
1150	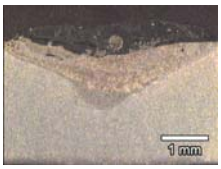	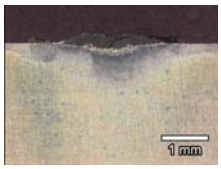

Fig .1 Weld bead profiles for various laser powers.

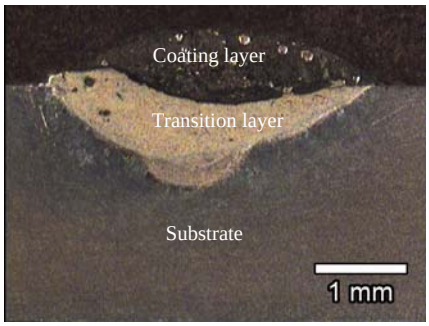

Fig.2 Schematic diagram showing three zones in weldment.

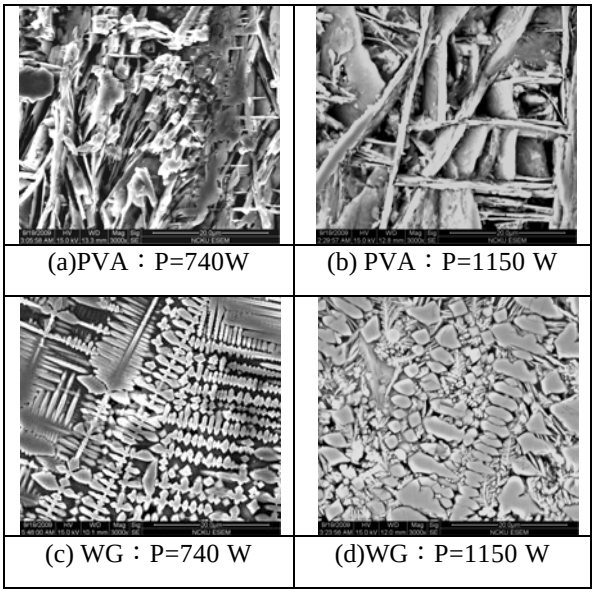

Fig .3 Morphology of coating layers processed at various conditions.

2. Ca/P ratio of coating layers

Figure 4 reveals the comparison of Ca/P (in wt.%) ratio of coating layers under various conditions. It can be seen clearly that the Ca/P ratio of the current FA-based coatings depends on both the choice of binder and the laser processing parameters. The Ca/P ratio is 3.6-5.8 in the PVA samples, whereas 13.6-15.1 is observed in the WG counterparts. Furthermore, the Ca/P ratio is increased with the output power. It is related to the P vaporization during heating at the high temperature. The higher output power generates a higher processing temperature and thus increases the P dissipation effect from the structure.

The difference Ca/P ratio of coating layers for both of the PVA and WG specimens is also most likely the result of the difference in the melting temperatures of the two binders. Due to the relatively low melting temperature of the PVA binder, the PVA content in the FA powder is vaporized and released completely into the surrounding atmosphere during the initial stages of the laser cladding process. However, the melting temperature of WG is close to that of FA (1525°C) and Ti-6Al-4V (1670°C). Therefore, if a binder with higher melting temperature is used, a higher laser power is expected for melting the FA-binder mixture, and this causes more P dissipation in the mean time. Another possibility could because of WG has a similar melting temperature with FA, and therefore would be melted around the same temperature region. When the WG binder was vaporized from the molten pool, it stimulated the agitation of the molten pool, and hence helped the P dissipation. [17,18].

Chien [18] coated HA on Ti-6Al-4V via similar technique shown above. However, the Ca/P ratio of the FA samples acquired in the study has a much lower value than those HA ones from Chien. This also indicates FA is more stable than HA under the same laser processing condition. This is probably because F ion can help to immobilize Ca and P ions and thus stabilize the Ca/P ratio of the structure [12].

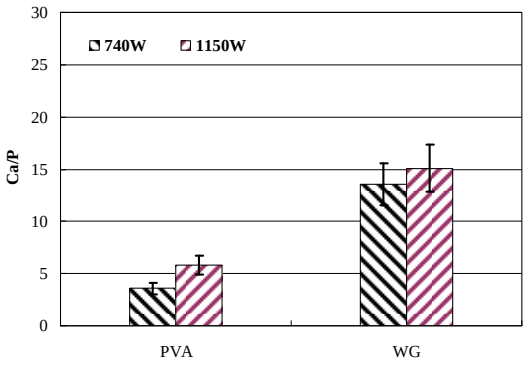

Fig.4 Comparison of Ca/P values of coating layers for various laser powers.

3. The phase analysis

Figure 5 shows the XRD spectrum of the coating layers. It reveals that the coating layer of the samples is mainly composed of FA, $CaTiO_2$, Al_2O_3 and $Ca_3(PO_4)_2$ phases, and they are all biocompatible. $CaTiO_2$ was combined from FA and Ti-6Al-4V, and $Ca_3(PO4)_2$ was decomposed from FA at a temperature higher than 1057°C [17]. It is found that $Ca_3(PO_4)_2$ has a highest peak among others in the WG sample, whereas FA is the highest one in the PVA counterpart. This is supposed that WG has a higher melting temperature than PVA, and a higher laser energy is required for the melt of the FA-WG mixture. Therefore, a relatively higher portion of $Ca_3(PO_4)_2$ was decomposed from FA in the WG sample, and a larger portion of FA phase was preserved in the PVA counterpart.

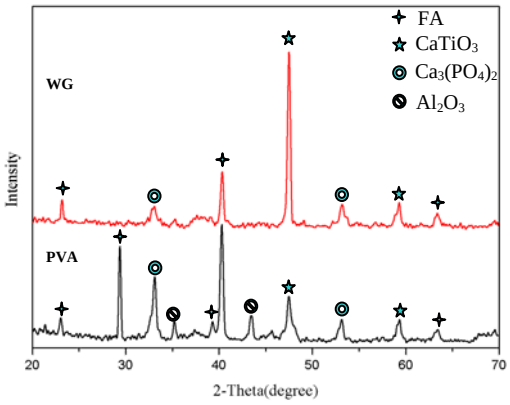

Fig.5 XRD analysis of the coating layers for different binders .(740W)

4. Hardness evaluation

Figure 6 presents the Vickers microhardness profiles of the various weld beads from the coating layer, transition layer and then into Ti-6Al-4V substrate. It can be seen clearly that the transition layer has a far higher hardness than either the substrate or the coating layer in all specimen. In addition, the WG sample has a relatively higher hardness than the PVA one in the transition layer region under the same experimental conditions. In the study, the EDS analysis revealed that Si was found in the transition layer of WG sample from the burnout of WG binder (Figure 7). Some Si-based compounds may help to the increase of the hardness and the strength of the structure.

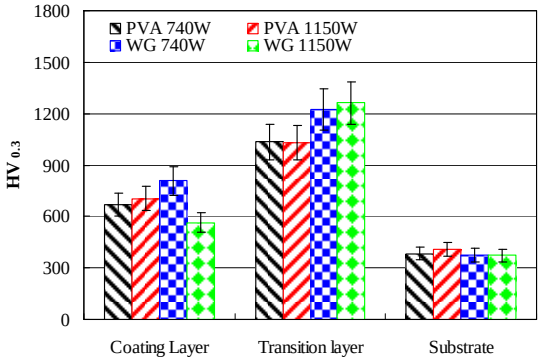

Fig.6 Vickers hardness profiles of weld beads from central coating layer, to transition layer, to substrate for various laser powers.

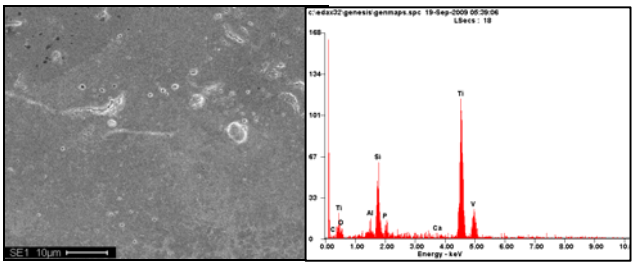

Fig.7 Transition layer's microstructure and EDS analysis of WG sample.

Conclusion

1. The coating layer was composed by a coral- and dendrite-like structure in the PVA sample; whereas dendrite structure was mainly found in the WG counterpart. The microstructure of the layers was getting coarser with the increase of output power.

2. The Ca/P ratio measurements reveal that WG sample has a significant higher value than the PVA sample under the same processing conditions. It is supposed that when a binder with higher melting temperature is used, a higher laser power is expected for melting the FA-binder mixture, and this causes more P dissipation in the mean time.

3. The XRD analysis reveal that the coating layer of the samples is mainly composed of FA, $CaTiO_2$, Al_2O_3 and $Ca_3(PO_4)_2$ phases. It is found that $Ca_3(PO_4)_2$ has a highest peak among others in the WG sample, whereas FA is the highest one in the PVA counterpart.

4. The Vickers microhardness measurements indicate that the transition layer has a far higher hardness than either the substrate or the coating layer in all specimen, and the WG sample has a relatively higher hardness than the PVA one in the transition layer region under the same experimental conditions.

Acknowledgements

The authors are grateful to the National Science Council for the financial support (grant number: NSC98-2815-C-218-007-E).

References

[1] C. Egrun, R. Doremus and W. Lanford (2003) .“Hydroxylapatite and titanium interfacial reaction”, *J. Biomed. Mater. Res. A*, 65, pp.336-343.

[2] E. Chang, W.J. Chang, B.C. Wang and C.Y. Yang (1997). “Plasma spraying of zirconia-reinforced hydroxyapatite composite coatings on titanium: Part I Phase, microstructure and bonding strength”, *Journal of Materials Science: Materials in Medicine* , 8(4), pp. 193-200 .

[3] O. Blind, L.H. Klein, B. Dailey and L. Jordan (2005). “Characterization of hydroxyapatite films obtained by pulsed-laser deposition on Ti and Ti-6Al-4V substrates”, *Dental Materials*, pp. 1017-1024.

[4] W. Suchanek and M. Yoshimura (1998). “ Processing and properties of hydroxyapatite-based biomaterials for use as hard tissue replacement implants ”,*Rev. J .Mater. Rs.* , 13, pp.94–117.

[5] T.F. Hong, Z.X. Guo and R. Yang (2008).” Fabrication of Porous Titanium Scaffold Materials by a Fugitive Filler Method”, Journal of Materials Science: Materials in Medicine, 19, 3489-3495,2008

[6] X. Zheng, M. Huang and C. Ding (2000). “Bond strength of plasma-sprayed hydroxyapatite/Ti composite coatings”, *Biomaterials*, pp. 841-849.

[7] K. Hing, S. Best and W. Bonfield (1999) “Hydroxyapatite and fluorapatite coatings for fixation of weight loaded implants” , *J. Mater. Sci. Mater. Med.*, 10, pp.135.

[8] J. I. Huaxia and P. M. Marquis (1993). “Sintering Behavior of Hydroxyapatite with 20wt% Al_2O_3 ” , *Journal of Materials Science*, 28, pp. 1941-1945.

[9] J. Zhou, X. Zhang, J. Chen, S. Zeng, and K. de Groot (1993). “High Temperature Characteristics of Synthetic Hydroxyapatite”, *J. Mater. Sci. Mater. Med.*, 4 , pp.83-85.

[10] Nenad Ignjatovie, Simonida Tomic, Momcilo Dakic, Miroslav Miljkovie, Milenko Plavsic, and Dragan Uskokovic (1999). “Synthesis and properties of hydroxyapatite/poly-L-lactide composite biomaterials” ,*Biomaterials*, 20, pp.809.

[11] Kinnari A. Bhadang and Kaarlis A. Gross (2004) , “Influence of fluorapatite on the properties of thermally sprayed hydroxyapatite coatings” ,*Biomaterials*, 25, pp.4935-4945.

[12] Foued Ben Ayed and Jamel Bouaziz (2008). “Sintering of tricalcium phosphate–fluorapatite composites by addition of alumina”, *Ceramics International*, 34, pp. 1885–1892.

[13] American Ceramic Society (1983). “Phase Diagrams for Ceramists”, *Washington DC*, 5, pp.321-322.

[14] L. Gineste, M. Gineste, X. Ranz, A. Ellefterion, A. Guihem, N. Rouquet and P. Frayssinet (1999). “Degradation of hydroxyapatite,fluorapatite and fluorhydroxyapaite coatings of dental implants in dogs”, *J. Biomed. Mater. Res.*, 48, pp.224-234.

[15] G. Wu, W.G. Zhang and C.T. Wang (2007). ”Tribological properties of PVA-H/HA composiyes”, *Tribology* , pp.214-218 .

[16] C.Z. Chen , D.G. Wang , P. Xu,, Q.H Bao., L. Zhang and T.Q. Lei (2004). “ Microstructure of laser cladding hydroxyapatite bioceramic gradient coatings”, *Chinese Journal of Lasers*, pp.1021-1024.(in China)

[17] D.G. Wang, C.Z. Chen, J. Ma and G. Zhang (2008).“In situ synthesis of hydroxyapatite coating by laser cladding” , *Colloids and Surfaces B: Biointerfaces*, 66 , pp.155–162.

[18] C.S. Chien, T.J. Han, T.F. Hong, T.Y. Kuo and T.Y.Liao, (2009), “Effects of different adhesive of hydroxyapatite power on weld morphology, Ca/P value and hardness of cladding layer by Nd-YAG deposition on Ti-6Al-4V substrate”, *Materials Transactions*, 50(2). (in press)